Thermomechanical Threshold of Laser Action on the Tympanic Membrane while Maintaining Its Structure

Olga I. Baum[1*], Ekaterina M. Kasianenko[1], Anna V. Zolotova[1,2], Mikhail V. Svistushkin[1,2], and Natalia B. Serejnikova[3]

[1] National Research Centre "Kurchatov Institute", 1 Kurchatov sq., Moscow 123182, Russian Federation
[2] Department of Ear, Nose and Throat Diseases, Federal State Autonomous Educational Institution of Higher Education I.M. Sechenov First Moscow State Medical University of the Ministry of Health of the Russian Federation (Sechenov University), 8 Trubetskaya str., Moscow 119048, Russian Federation
[3] Institute for Regenerative Medicine, Federal State Autonomous Educational Institution of Higher Education I.M. Sechenov First Moscow State Medical University of the Ministry of Health of the Russian Federation (Sechenov University), 8 Trubetskaya str., Moscow 119048, Russian Federation
*e-mail: baumolga@gmail.com

Abstract. Laser-induced modification of the structure and properties of biological tissues is a novel and rapidly advancing approach used for tissue reconstruction without causing destruction or coagulation of the biological material. This work is devoted to determining the threshold values of laser exposure parameters on the tissue of the tympanic membrane (TM) while preserving its integrity and structure. The findings aim to facilitate the extrapolation of principles from established laser-based technologies to new biological tissue types, notably those where cells exist predominantly in a state of normoxia. This work is the first step in the development of a new laser technology − laser regeneration of the TM. In this work, using computer modeling, temperature fields and thermal stress fields, the values of which are close to known values, which have a positive effect on cell proliferation and matrix synthesis, were found. Two laser modes selected for the *in vivo* experiment made it possible to determine the acceptable range of effects on the TM under conditions of maintaining its integrity and to find the threshold for detachment of the TM epithelium while maintaining the structure of its deeper layers.

Keywords: infrared laser; temperature field; thermomechanical stress; tympanic membrane.

Paper #9350 received 1 Sep 2025; revised manuscript received 21 Sep 2025; accepted for publication 22 Sep 2025; published online 2 Oct 2025. doi: 10.18287/JBPE25.11.030306.

1 Introduction

Laser-induced modification of the structure and properties of biological tissues is a novel and rapidly advancing approach used for tissue reconstruction without causing destruction or coagulation of the biological material. The primary indicator of treatment efficacy is the preservation of the tissue's functional characteristics. Prominent examples of such technologies include the method for laser treatment of laryngeal stenosis, which has been developed and successfully implemented into clinical practice [1−3], as well as a technique for laser-based regeneration of joint cartilage [4−10], the efficacy of which has been corroborated by cellular studies [2, 11−13]. This study focuses on identifying the threshold parameters of laser exposure on tympanic membrane (TM) tissue, ensuring the preservation of its structural integrity. The results are intended to support the translation of established laser-based methodologies to novel biological tissues, particularly those in which cells predominantly exist under normoxic conditions.

TM perforation remains a common clinical problem worldwide. Perforations can be classified as acute or chronic. While acute TM perforations typically demonstrate a tendency toward spontaneous closure within 7–10 days, the presence of a chronic defect predisposes patients to middle ear infections and may result in significant hearing impairment. This, in turn,

compromises the patients' quality of life, restricts their ability to communicate and exchange information, and reduces their social activity [14−15].

Currently, alternative methods for closing TM perforations are emerging to replace traditional surgical approaches, such as tympanoplasty and myringoplasty. These include the use of various scaffolds, growth factors, and stem cells. The most common treatment strategies involve a combination of these tissue-engineered materials [16−20].

Currently, laser therapy for tympanic membrane perforation is used only as an adjunctive surgical tool. Studies show that CO_2 lasers can be used for precise de-epithelialization of the perforation edges, facilitating subsequent closure of the lesion. Wani et al. (2021) compared the results of CO_2 laser myringoplasty with traditional tympanoplasty and demonstrated perforation closure in 80% of cases, which is slightly lower than with standard surgery (90–94%). However, the laser minimized the impact on surrounding tissue [21].

Combining laser treatment with biomaterials also demonstrates high efficacy. Kuroda et al. (2024) used the OtoLAM CO_2 laser to prepare perforation margins, followed by application of a two-layer collagen sponge (Terudermis). In this study, the overall perforation closure rate was 69.7%, with the highest success rate observed in traumatic injuries (84.6%) [22].

One of the important findings is the identification of latent epithelial stem or progenitor cells within the TM [23−25]. It has been suggested that their activation contributes to the regeneration of the damaged TM. We hypothesize that laser irradiation may serve as a stimulatory factor for initiating regenerative processes of TM perforation. In the literature, there is a study in which TM tissues with post-traumatic perforations were irradiated using lasers with wavelengths of 630 nm and 860 nm. These processes resulted in the restoration of the TM with adequate proliferation of connective tissue and without excessive formation of fibrous tissue, in contrast to the control group (where laser treatment was not applied) [26].

It has been experimentally demonstrated that low-intensity laser irradiation is an effective tool in regenerative medicine for inducing proliferative and differentiation processes in mesenchymal stromal cells (such as osteoblasts, chondrocytes, and fibroblasts) and progenitor cells [27].

Laser irradiation exerts a complex effect on biological tissues, manifesting not only at the cellular and molecular levels but also at the organ level, where it promotes the normalization of metabolic processes and improves microcirculation. In this context, regeneration is considered as a natural response of living tissue to damage. However, the intensity of reparative processes, their dynamics, and the characteristics of the newly formed tissue are directly dependent on the parameters of the external stimulus [10, 28].

Cells of the organism exhibit high sensitivity to changes in the microenvironment, including temperature fluctuations and mechanical stresses. Laser irradiation, modulated in time and space, is capable of generating pulsed-periodic tissue heating, which induces locally heterogeneous thermal expansion and generates pulsating fields of mechanical stress. These controlled factors create specific conditions for cells, enhancing their proliferative activity and stimulating their biosynthetic functions. Consequently, laser exposure can be considered as a tool for the targeted activation of tissue healing and regeneration processes [2].

Modern studies show that medium-intensity laser radiation can have a combined effect on mesenchymal stem cells (MSCs), combining photobiomodulatory and thermal effects. A number of studies have demonstrated that such a combination has a pronounced stimulating effect on the proliferation and colony-forming activity of MSCs. In particular, it was shown that the fragmental (fractional) thermal effect of laser radiation with a wavelength of $\lambda = 1.56$ μm on the BM of rats *in vivo* makes it possible to increase the content of MSCs by two times [29], and when using a wavelength of 980 nm with simultaneous exposure to light and heat, the number of colonies increases several times compared to the control and more than 3 times compared to isolated thermal exposure [30, 31].

An important tool in this field is computer modeling, which allows for the establishment of therapeutic ranges of radiation parameters. Within these ranges, the desired biological response is achieved while avoiding undesirable side effects. Such models are actively used in research, particularly on hard-to-access biological tissues, thereby reducing the scope of *ex vivo* and *in vivo* experiments [8, 32]

Thus, the objective of this study was first to theoretically determine the range, and subsequently, under *in vivo* experimental conditions, to establish the threshold values of laser exposure parameters on the TM tissue while preserving its integrity and structure, followed by histological confirmation.

2 Materials and Methods

2.1 Theoretical Modeling

The theoretical model is based on the heat conduction equation with a volumetric heat source $G(x,y,z,\tau)$, generated by laser radiation and attenuating with depth according to the Bouguer-Lambert-Beer law with an effective absorption coefficient κ

$$\frac{\partial T(x,y,z,\tau)}{\partial \tau} = a\Delta T(x,y,z,\tau) + G(x,y,z,\tau), \quad (1)$$

where a is the thermal diffusivity coefficient. The density of the incident energy flux on the cross-sectional surface of the cartilaginous tissue exhibits a spatial distribution corresponding to a Gaussian profile, with an effective beam radius $r_0(x)$, that accounts for beam divergence in the transverse direction as it propagates through the media along the x-axis.

$$G(x,y,z,\tau)=P(\tau)\exp\left(-\frac{y^2+z^2}{r_0^2(x)}\right)\frac{\kappa\exp(-\kappa x)}{c\rho}, \quad (2)$$

where $P(\tau)$ denotes the time-dependent laser power, c – the specific heat capacity, ρ – the density. At the interfaces between different media, the boundary condition of constant heat flux density was applied. Temperature gradients give rise to thermoelastic stresses, which can be derived for each temperature profile.

For theoretical consideration, pulse-periodic modes with a pulse duration of 100 ms and a repetition duration of 1 Hz were selected. Dynamics of the maximum temperature on the front and back surfaces of samples with a thickness of 100, 150 and 200 μm were constructed. The irradiation power was from 0.1 to 0.7 W. The data for cartilage were chosen as constants describing the model biological environment, since thin autologous cartilage (100–200 μm) is, in terms of its comparative properties, an acoustically and mechanically adequate model of the native tympanic membrane (TM) [33–36].

Experimental studies [33, 34] and numerical modeling [35] confirm that grafts of this thickness do not have a significant effect on the transfer function and vibrational characteristics of the TM. Clinical data [36] demonstrate their effectiveness in tympanoplasty, providing biomechanical stability without compromising acoustic response. Thus, thin cartilage is justifiably used as an in vitro model for studying the biophysics of TM and testing reconstructive techniques.

In numerical modeling, for the moments of achievement the maximum temperature at the first and last pulses in the series of irradiation, temperature profiles were constructed on the front surface, which were then approximated by Gaussian axially symmetric functions $T(r)$, which led to the discovery of the components of the thermal stress tensor. Solving the thermoelastic problem under this irradiation geometry enables determination of the radial and angular components of the thermoelastic stress tensor, expressed as follows:

$$\sigma_r=\alpha E\left(\frac{1}{b^2}\int_0^b T(r)rdr-\frac{1}{r^2}\int_0^r T(r)rdr\right);$$
$$\sigma_\theta=\alpha E\left(-T(r)+\frac{1}{b^2}\int_0^b T(r)rdr+\frac{1}{r^2}\int_0^r T(r)rdr\right), \quad (3)$$

where b denotes the boundary of the integration domain with respect to the radial coordinate, α – the coefficient of thermal expansion, E – the elastic modulus, $T(r)$ – represents the Gaussian distribution of the temperature profile.

Using Eq. (3), the region of maximum deformations, determined by the difference between the angular and radial components, the maximum value of which has a decisive influence on the cell and its environment, have been calculated.

2.2 In vivo Experiment on Small Laboratory Animals

An experimental study was conducted on laser exposure at a wavelength of 1.56 μm with various power and time parameters on small laboratory animals, approved by the local ethics committee (protocol No. 10−24 dated 04/18/2024).

According to the literature, the chinchilla is an optimal experimental model for the middle ear. Rats and guinea pigs have a small diameter of the external auditory canal, which significantly complicates simultaneous manipulation with endoscope and instruments, or work under a microscope using two instruments [37]. The diameter of the external auditory canal chinchilla is enough for manipulations on the TM using a 4 mm rigid endoscope, which significantly improves the view compared to using microscopic equipment. The diameter of the TM of chinchilla is 7–10 mm. The structure of the TM and auditory ossicles is similar to humans [38–40]. Thus, adult male chinchillas weighing 500–700 g, aged 6 months, were chosen as an experimental model. Males were used due to the lower hormonal variability of males.

All manipulations were performed in a vivarium complex. Before anesthesia, the animals were fasted for 12 h. Then, the chinchillas of both groups were given general anesthesia by intramuscular administration of a solution of Zoletil at a dose of 10 mg/kg and Xylazine (dose 0.15 ml/kg), which corresponds to the minimum dosages used for short-term painful procedures. Before the administration of the drugs, a solution of Atropine sulfate (at a dose of 0.05 mg/kg of animal weight) was administered subcutaneously as premedication 15 min before.

After the animal was anesthetized, using a 0-degree rigid endoscope (Karl Storz, Germany) connected to the video camera console controller (Karl Storz), the TM was examined for its integrity and the absence of inflammation (Fig. 1, Fig. 2).

Fig. 1 Endoscopic examination of the TM.

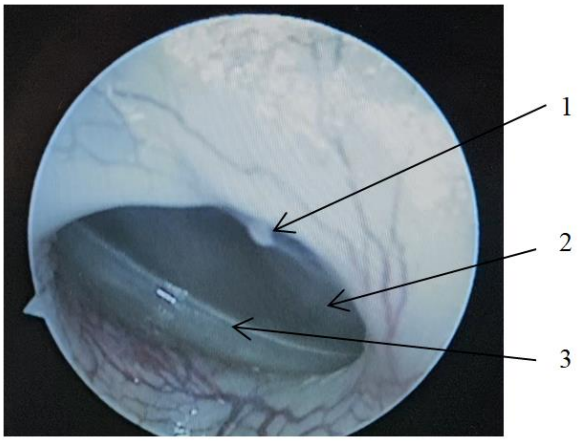

Fig. 2 Chinchilla's tympanic membrane viewed with an endoscope: 1 – umbo, 2 – anteroinferior quadrant of the tympanic membrane of the chinchilla, 3 – annulus tympanicus.

The next step was TM exposition to laser radiation (wavelength of 1.56 μm) using a 600 μm diameter fiber optic in the area of the annulus tympanicus and the umbo (Fig. 3). According to the literature, progenitor cells were found in the indicated areas, forming the TM's own regenerative potential [23–25]. Laser radiation was applied perpendicular to the surface of the tympanic membrane, at a distance of 1 mm from it.

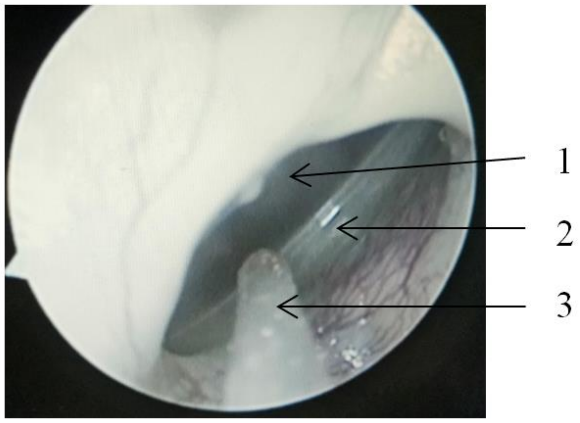

Fig. 3 The laser fiber is guided to the annulus tympanicus of the tympanic membrane: 1 – tympanic membrane, 2 – annulus tympanicus, 3 – optical fiber that delivers laser radiation.

Six animals were divided into 2 groups:

• group 1–3 chinchillas (6 ears), whose TM's were exposed to a laser with a wavelength of 1.56 μm and a power of 0.5 W, with pulses of 100 ms for a total duration of 15 s, power density 56 W/cm² (laser mode №1);

• group 2–3 chinchillas (6 ears), whose TM's were exposed to a laser with a wavelength of 1.56 μm and a power of 0.3 W, with pulses of 100 ms for a total duration of 30 s, power density 100 W/cm² (laser mode №2).

2.3 Control Otoendoscopy

After irradiation of the specified areas of the TM, control otoendoscopy was performed using an endoscope (Karl Storz, Germany).

After that all animals were then removed from the experiment.

Euthanasia was performed using an overdose of anesthetics, which, in accordance with the European Directive 2010/63/EU on the protection of animals used for scientific purposes, is included in the list of applicable methods of euthanasia for rodents. The use of injectable drugs is the fastest, most reliable and optimal method of euthanasia, as it does not cause pain or fear of the animal [41]. Material was taken only after confirmation of the animal's death (absence of pulse, breathing, absence of corneal reflex, inability to hear breathing and heartbeat using a phonendoscope).

2.4 Histological Examination

After the animal was removed from the experiment, the TM preparation was instrumentally isolated under the control of a Carl Zeiss microscope. The obtained samples were fixed in neutral formalin, decalcified in a Biodec R solution, embedded in paraffin, serial sections 4 μm thick were obtained every 50 μm, and stained with hematoxylin and eosin. The samples were studied using standard light microscopy and phase-contrast microscopy in a Leica DM 4000 B LED microscope (Leica Camera AG, Germany) with a Leica DFC 7000 T camera (Leica Camera AG, Germany).

3 Results and Discussion

Using a theoretical model in a numerical experiment for the time of reaching the maximum temperature on the first and last pulses in irradiation series differing in power and total duration, temperature profiles were constructed on the front surface of the irradiation, which were then approximated by Gaussian axisymmetric functions of the form $T(r)$, which made it possible to find the components of the thermal stress tensor. Using Eq. (3), the region of maximum thermal stresses was calculated, determined by the difference between the angular and radial components, the maximum value of which has a decisive influence on the cells and their environment.

Figure 4 shows the theoretical dynamics of the maximum temperature on the front surface of the samples in two modes selected for further *in vivo* experiments. Laser mode No. 1: power 0.5 W, total irradiation duration 15 s; laser mode No. 2: power 0.3 W, total irradiation duration 30 s.

It is shown that the temperature on the back surface of a 100 μm thick sample is lower than the temperature on the front surface by approximately 3%, and for a 200 μm thick sample by 6%. Thermal stresses were calculated for the front surface of the samples – from the side of incident radiation (Fig. 5).

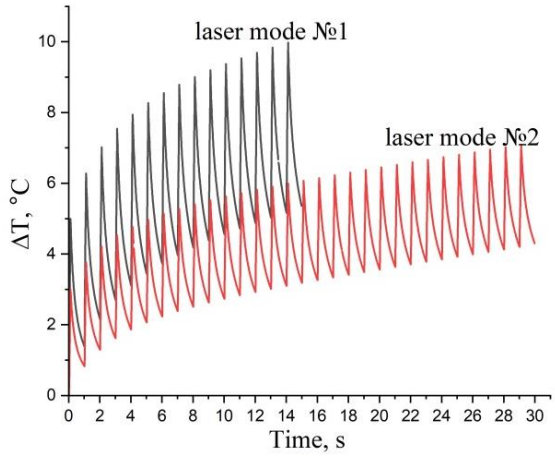

Fig. 4 Theoretical dynamics of change in maximum temperature during irradiation in two laser modes.

The approximation of the temperature profiles was substituted into the equation for the components of the thermal stress tensor and the values of the maximum thermal stresses at the moment of reaching the maximum temperature at the end of the first and last pulses with a duration of 100 ms for the two selected modes were found. Their profiles are shown in Fig. 6. With a power difference of 1.7 times and an irradiation duration of 2 times, the temperature maxima on the first and last irradiation pulses for a more powerful mode differed by 2 times, and for a more gentle one by 2.3 times. At the same time, the corresponding difference in the maximum values of thermal stresses was 1.5 and 1.47 times, which indicates that the dynamics of thermal stresses depend not so much on the absolute values of the temperatures achieved, but on the dynamics of the temperature field propagation.

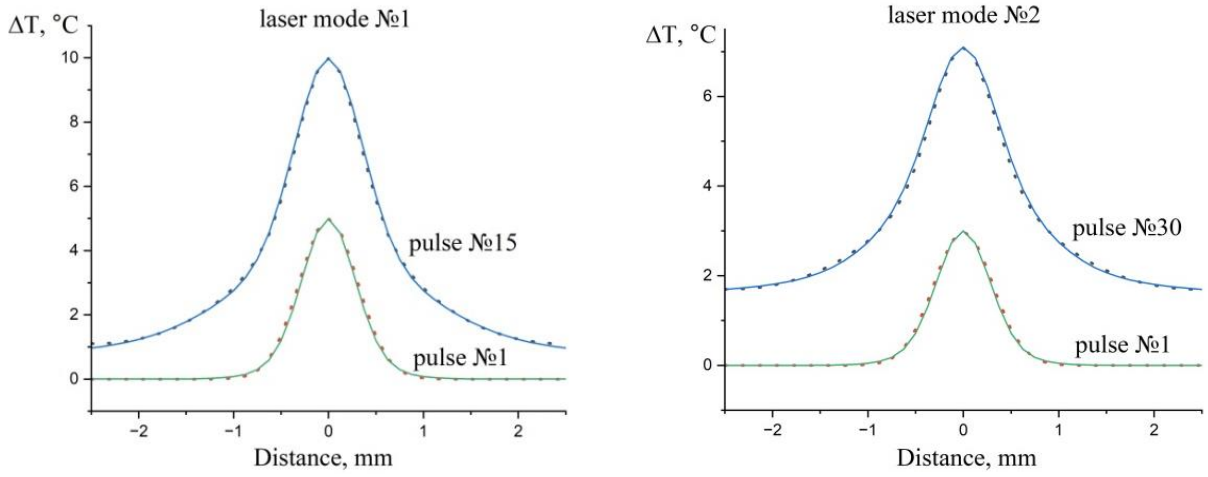

(a) (b)

Fig. 5 Theoretical temperature profiles in a direction perpendicular to the propagation of the light beam (points) and their approximation (lines) for two laser modes at the first and last pulses for two modes: (a) laser mode №1, (b) laser mode №2.

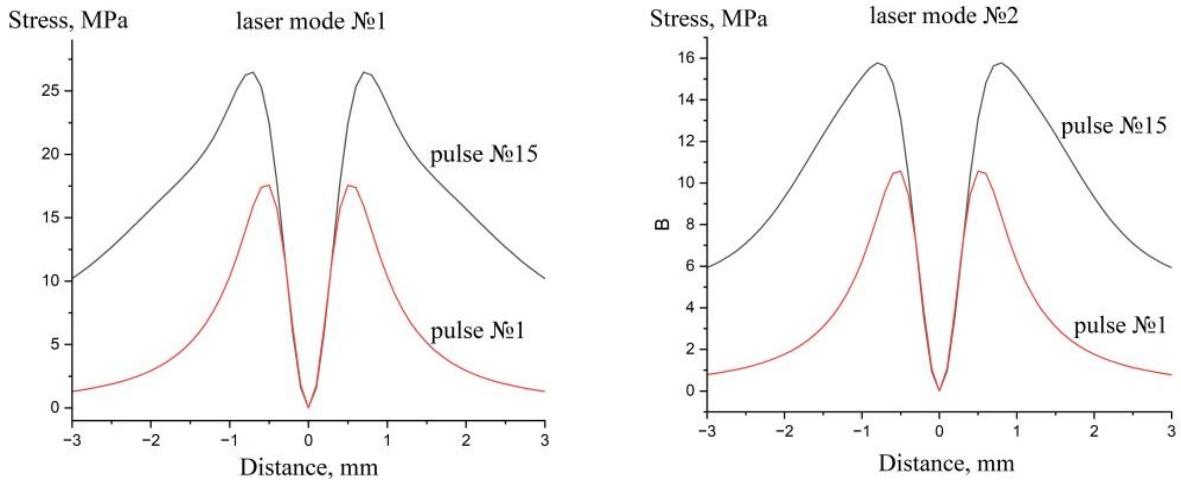

(a) (b)

Fig. 6 Thermal stress for two modes at the first and last pulse of the series: (a) laser mode №1, (b) laser mode №2.

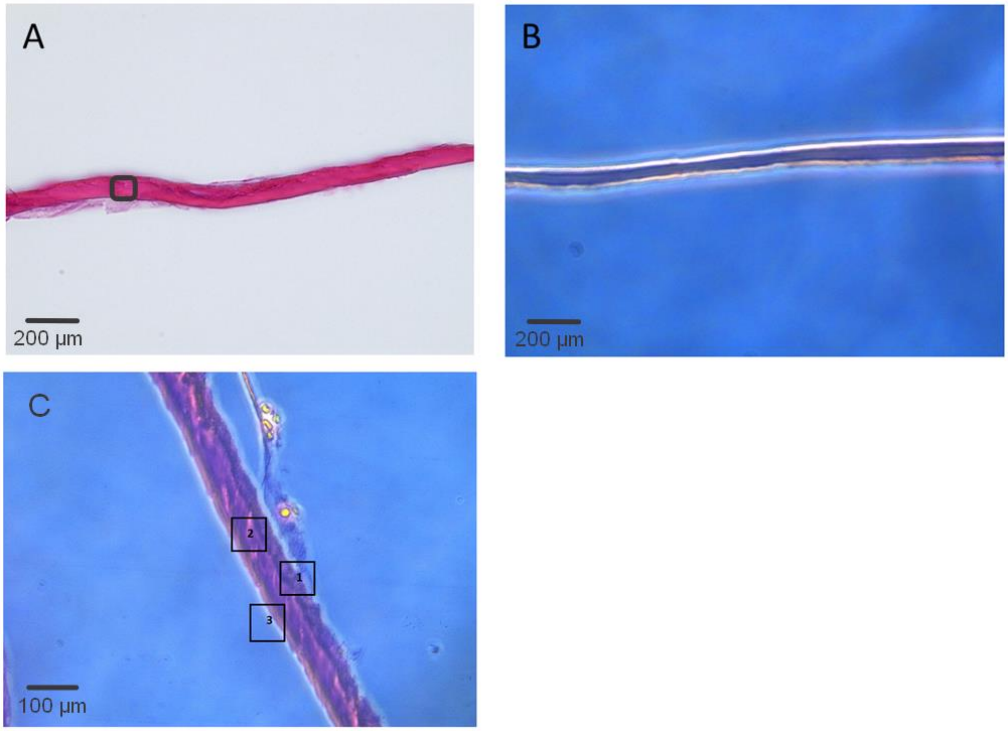

Fig. 7 Tympanic membrane, normal. (A) Hematoxylin and eosin staining. Magnification ×400. (B) Phase-contrast microscopy. Magnification ×400. (C) Phase contrast microscopy (magnification ×630): 1 − external layer (stratified squamous epithelium); 2 – fibrous layer (fibrous connective tissue); 3 − mucous layer (simple epithelium).

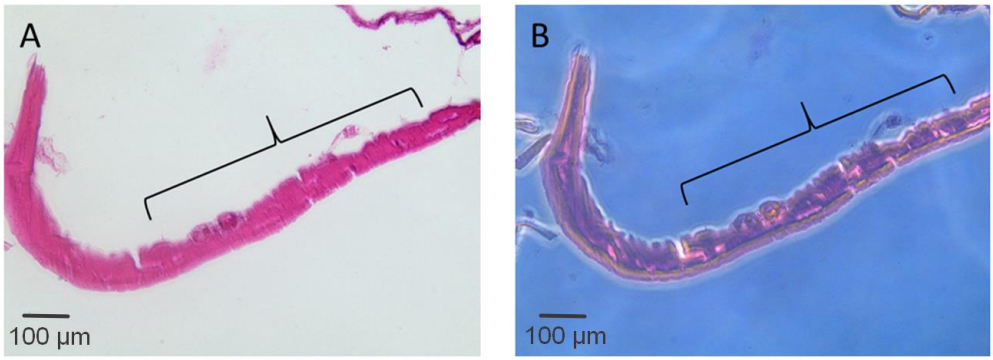

Fig. 8. Tympanic membrane, irradiated area of group 1. Magnification ×630. (A) Hematoxylin and eosin. (B) Phase-contrast microscopy. The curly bracket indicates the laser exposure zone.

The region of maximum thermal stresses has a ring shape and is located on the periphery of the laser spot, moving away from the axis of laser action with each subsequent pulse. Using numerical modeling, two laser action modes were selected from the studied range of modes, in which the values of thermal stresses are close to the values that have a positive effect on cell proliferation and matrix synthesis [2].

Both modes presented above were selected for further *in vivo* experiments, and the irradiation geometry was also selected based on the calculations performed. Thus, in the subsequent *in vivo* experiment, laser radiation was delivered to the target area using quartz optical fiber with a core diameter of 600 μm. The fiber optic tip was positioned in close proximity to the surface of the TM, but excluding physical contact with the tissue. The power density in the treatment zone varied in the range from 56 to 100 W/cm². This power density was chosen taking into account the angular location of the TM inside the chinchilla's ear canal and the impossibility of perpendicularly feeding the optical fiber to the TM surface.

After laser irradiation, control otoendoscopy did not reveal any damage to the TM tissues in any case. During the histological examination, the first stage was to study the areas of the TM outside the irradiation zone. The tissue of the chinchilla TM outside the irradiation points has a normal structure: a layer of multilayer squamous epithelium, a layer of loose fibrous connective tissue, a layer of simple epithelium (Fig. 7). The three-layer structure of the TM is especially clearly visible with phase-contrast microscopy (Fig. 7C).

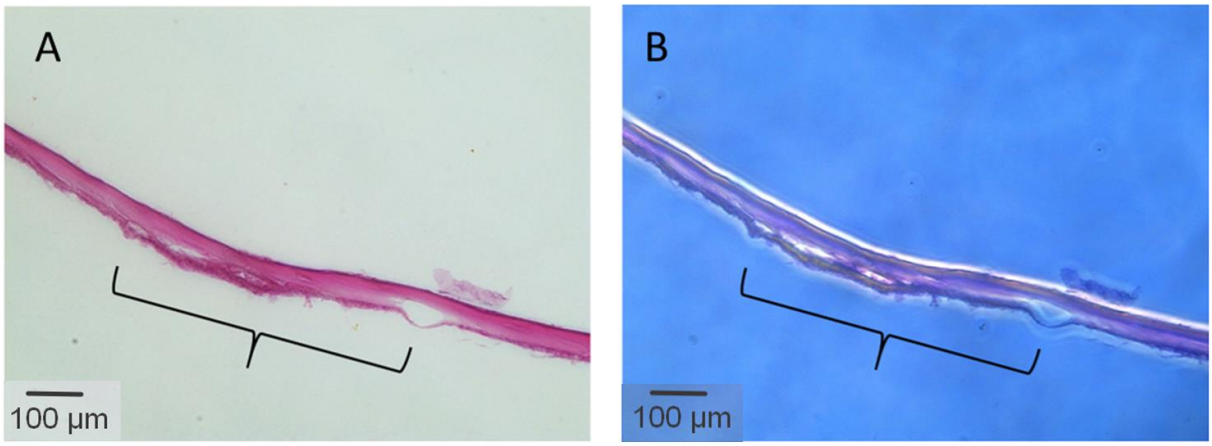

Fig. 9 Tympanic membrane, irradiated area of group 2. (×630). (A) Hematoxylin and eosin. (B) Phase-contrast microscopy. The curly bracket indicates the area of exfoliating epithelium.

The second stage involved studying the irradiated areas of the TM tissue in groups 1 and 2. In group 1 (laser mode №1), the irradiated areas had a foamy structure and were vacuolated, which may indicate the initial stage of laser vaporization (Fig. 8), in which the stratified squamous epithelium is damaged (coagulation necrosis).

In group 2 (laser mode №2), a zone of peeling epithelium is visible in the irradiated areas, which at the same time retains its normal structure (Fig. 9).

4 Conclusions

Based on the theoretical model presented in the work, the dynamics and profiles of the temperature field on the front surface of the irradiated sample and the corresponding profiles of the thermal stress field were constructed. Accordingly, for the moment of reaching the maximum temperature at the end of each pulse with a duration of 100 ms, the thermal stress fields also reach a maximum. The area of maximum thermal stresses has a ring shape and is located on the periphery of the laser spot, moving away from the axis of laser action with each subsequent pulse. Using computer modeling, laser action modes were found in which the values of thermal stresses are close to the values that have a positive effect on cell proliferation and matrix synthesis [2].

Two modes selected for the *in vivo* experiment and differing from each other in power by about 1.7 times and in the total duration of irradiation by 2 times, made it possible to determine the acceptable range of action on the BP under conditions of maintaining its integrity and to find the threshold for detachment of the BP epithelium while maintaining the structure of its deeper layers.

Acknowledgements

The study was supported by the Russian Science Foundation, grant No. 25-15-00341.

Disclosures

All authors declare that there is no conflict of interest in this paper.

References

1. V. M. Svistushkin, S. V. Starostina, L. V. Selezneva, O. I. Baum, E. N. Sobol, Yu. M. Alexandrovskaya, and A. V. Starostin, "The use of modified autografts for plastic closure of laryngotracheal defects: An experimental study," Farmateka 27(5), 72–76 (2020).
2. Yu. M. Alexandrovskaya, O. I. Baum, A. B. Shekhter, E. V. Petersen, O. A. Tiflova, A. K. Dmitriev, V. A. Ulyanov, V. M. Svistushkin, L. V. Selezneva, and E. N. Sobol, "Mechanisms of laser activation of chondrocytes in osteoarthritis healing," Laser Physics Letters 15(8), 085601 (2018).
3. O. I. Baum, Y. M. Soshnikova, E. N. Sobol, A. Ya. Korneychuk, M. V. Obrezkova, V. M. Svistushkin, O. K. Timofeeva, and V. V. Lunin, "Laser reshaping of costal cartilage for transplantation," Lasers in Surgery and Medicine 43(6), 511–515 (2011).
4. Yu. M. Alexandrovskaya, O. I. Baum, A. A. Sovetsky, A. L. Matveyev, L. A. Matveev, E. N. Sobol, and V. Y. Zaitsev, "Spatially-resolved slow dynamics of strains due to residual stresses in cartilaginous implants visualized by phase-sensitive optical coherence tomography," Proceedings of SPIE 11641, 116410S (2021).
5. E. M. Kasyanenko, A. I. Omelchenko, and O. I. Baum, "Deformation response of biological phantoms and cartilage tissue under laser irradiation," Optics and Spectroscopy 131, 1000–1005 (2023).

6. Y. M. Alexandrovskaya, O. I. Baum, A. V. Yuzhakov, V. M. Svistushkin, A. V. Buzmakov, Y. S. Krivonosov, B. S. Roshchin, and D. A. Zolotov, "Infrared laser effect on healthy and ossified costal cartilage: The development of stable load-bearing autoimplants," Lasers in Surgery and Medicine 53(2), 275–283 (2021).
7. V. Y. Zaitsev, A. L. Matveyev, L. A. Matveev, G. V. Gelikonov, D. V. Shabanov, A. A. Sovetsky, A. I. Omelchenko, O. I. Baum, and A. Vitkin, "Optical coherence elastography assesses tissue modifications in laser reshaping of cornea and cartilages," Proceedings of SPIE 10496, 104960G (2018).
8. E. Sobol, O. Baum, A. Shekhter, A. Guller, and A. Baskov, "Laser-induced micropore formation and modification of cartilage structure in osteoarthritis healing," Journal of Biomedical Optics 22(9), 091515 (2017).
9. O. I. Baum, Yu. M. Soshnikova, A. I. Omelchenko, and E. N. Sobol, "Nanoparticles for diagnostics and laser medical treatment of cartilage in orthopaedics," Proceedings of SPIE 8595, 85951K (2013).
10. E. Sobol, A. Shekhter, A. Guller, O. Baum, and A. Baskov, "Laser-induced regeneration of cartilage," Journal of Biomedical Optics 16(8), 080902 (2011).
11. C. R. Tim, C. C. S. Martignago, L. Assis, L. M. Neves, A. L. Andrade, N. C. Silva, N. Parizotto, K. Z. Pinto, and A. C. Rennó, "Effects of photobiomodulation therapy in chondrocyte response by in vitro experiments and experimental model of osteoarthritis in the knee of rats," Lasers in Medical Science 37(3), 1677–1686 (2022).
12. Yu. M. Soshnikova, O. I. Baum, E. M. Shcherbakov, A. I. Omelchenko, A. B. Shekhter, V. V. Lunin, and E. N. Sobol, "Laser radiation effect on chondrocytes and intercellular matrix of costal and articular cartilage impregnated with magnetite nanoparticles," Lasers in Surgery and Medicine 47(3), 243–251 (2015).
13. E. Sobol, N. Vorobieva, O. Baum, A. Shekhter, and A. Guller, "Is it possible to perform laser reshaping without dramatic effect on chondrocytes," Lasers in Surgery and Medicine 43(S23), 911 (2011).
14. Z. Hussain, R. Pei, "Necessities, opportunities, and challenges for tympanic membrane perforation scaffolding-based bioengineering," Biomedical Materials 16(3), 032001 (2021).
15. S. Kanemaru, H. Umeda, Y. Kitani, T. Nakamura, S. Hirano, and J. Ito, "Regenerative treatment for tympanic membrane perforation," Otology & Neurotology 32(8), 1218–1223 (2011).
16. X. Zhao, J. Zhang, P. Tian, and X. Cui, "The latest progress of tympanic membrane repair materials," American Journal of Otolaryngology 43(5), 103408 (2022).
17. M. Aleemardani, Z. Bagher, M. Farhadi, H. Chahsetareh, R. Najafi, B. Eftekhari, and A. Seifalian, "Can tissue engineering bring hope to the development of human tympanic membrane?," Tissue Engineering Part B: Reviews 27(6), 572–589 (2021).
18. R. Kaboodkhani, D. Mehrabani, A. Moghaddam, I. Salahshoori, and H. A. Khonakdar, "Tissue engineering in otology: a review of achievements," Journal of Biomaterials Science 35(7), 1105–1153 (2024).
19. E E. A. Harvey, W. Hong, E. J. Sheehy, R. J. do Amaral, P. Khampang, C. L. Runge, C. O'Leary, F. J. O'Brien, and J. E. Kerschner, "Chronic tympanic membrane perforation repair with a collagen-based scaffold: An *in vivo* model," International Journal of Pediatric Otorhinolaryngology 176, 111807 (2024).
20. R. Najafi, F. Yazdian, M. Pezeshki-Modaress, M. Aleemardani, H. Chahsetareh, S. Hassanzadeh, M. Farhadi, and Z. Bagher, "Fabrication and optimization of multilayered composite scaffold made of sulfated alginate-based nanofiber/decellularized Wharton's jelly ECM for tympanic membrane tissue engineering," International Journal of Biological Macromolecules 253, 127128 (2023).
21. I. Singh, B. S. Patil, and M. Z. Akhtar, "A study to compare the outcomes of CO2 laser assisted myringoplasty versus conventional type1 tympanoplasty in small central tympanic perforations," International Journal of Otorhinolaryngology and Head and Neck Surgery 7(5), 809–814 (2021).
22. K. Kuroda, N. Kuroda, "Statistical evaluation of 231 ears that received tympanic membrane perforation closure using OtoLAM and Terudermis," International Journal of Practical Otolaryngology 07(01), e1–e8 (2024).
23. S. W. Kim, J. Kim, H. Seonwoo, K. J. Jang, Y. J. Kim, H. J. Lim, K. T. Lim, C. Tian, J. H. Chung, and Y. H. Choung, "Latent progenitor cells as potential regulators for tympanic membrane regeneration," Scientific Reports 5, 11542 (2015).
24. L. J. Liew, A. Y. Wang, and R. J. Dilley, "Isolation of epidermal progenitor cells from rat tympanic membrane," in Progenitor Cells. Methods in Molecular Biology, M. V. Joglekar, A. A. Hardikar (Eds.), Springer New York, 247–255 (2019).
25. J. Knutsson, M. von Unge, and H. Rask-Andersen, "Localization of progenitor/stem cells in the human tympanic membrane," Audiology and Neurotology 16(4), 263–269 (2011).
26. S. Maleki, S. K. Kamrava, D. Sharifi, M. Jalessi, A. Asghari, S. Ghalehbaghi, and P. Yazdanifard, "Effect of local irradiation with 630 and 860 nm low-level lasers on tympanic membrane perforation repair in guinea pigs," The Journal of Laryngology & Otology 127(3), 260–264 (2013).
27. A. N. Pereira, C. de P. Eduardo, E. Matson, and M. M. Marques, "Effect of low-power laser irradiation on cell growth and procollagen synthesis of cultured fibroblasts," Lasers in Surgery and Medicine 31(4), 263–267 (2002).
28. E. N. Sobol, T. E. Milner, A. B. Shekhter, O. I. Baum, A. E. Guller, N. Yu. Ignatieva, and V. V. Lunin, "Laser reshaping and regeneration of cartilage," Laser Physics Letters 4(7), 488–502 (2007).

29. R. K. Chailahyan, Y. V. Gerasimov, A. P. Sviridov, A. V. Kondjurin, A. H. Tambiev, and V. N. Bagratishvili, "Effect of IR laser radiation on the multipotent mesenchymal stromal stem cells of rat marrow *in vivo*," Russian Journal of Immunology 3(3–4), 333–337 (2009). [in Russian]
30. R. K. Chailakhyan, A. G. Grosheva, N. N. Vorob'eva, A. P. Sviridov, and V. I. Yusupov, "Laser thermo-photobiomodulation of bone marrow mesenchymal stem cells," Bulletin of Experimental Biology and Medicine 174(4), 523–526 (2023).
31. R. Chailakhyan, A. Grosheva, N. Vorobieva, V. Yusupov, and A. Sviridov, "Combined light and thermal stimulation of bone marrow stem cells," Journal of Lasers in Medical Sciences 15, e8 (2024).
32. O. I. Baum, "Temperature control system for laser reshaping of nasal septum," Journal of Instrument Engineering 58(10), 847–854 (2015). [in Russian]
33. T. Zahnert, K. B. Hüttenbrink, D. Mürbe, and M. Bornitz, "Experimental investigations of the use of cartilage in tympanic membrane reconstruction," Otology & Neurotology 21(3), 322–328 (2000).
34. A. A. Aarnisalo, J. T. Cheng, M. E. Ravicz, and J. J. Rosowski, "Middle ear mechanics of cartilage tympanoplasty evaluated by laser holography and vibrometry," Otology & Neurotology 30(8), 1209–1214 (2009).
35. C. F. Lee, J. H. Chen, Y. F. Chou, L. P. Hsu, P. R. Chen, and T. C. Liu, "Optimal graft thickness for different sizes of tympanic membrane perforation in cartilage myringoplasty: a finite element analysis," The Laryngoscope 117(4), 725–730 (2007).
36. D. Mürbe, T. Zahnert, M. Bornitz, and K. B. Hüttenbrink, "Acoustic properties of different cartilage reconstruction techniques of the tympanic membrane," The Laryngoscope 112(10), 1769–1776 (2002).
37. A. Y. Wang, Y. Shen, J. T. Wang, P. L. Friedland, M. D. Atlas, and R. J. Dilley, "Animal models of chronic tympanic membrane perforation: a 'time-out' to review evidence and standardize design," International Journal of Pediatric Otorhinolaryngology 78(12), 2048–2055 (2014).
38. P. A. Vrettakos, S. P. Dear, and J. C. Saunders, "Middle ear structure in the chinchilla: a quantitative study," American Journal of Otolaryngology 9(2), 58–67 (1988).
39. P. L. Santa Maria, M. D. Atlas, and R. Ghassemifar, "Chronic tympanic membrane perforation: a better animal model is needed," Wound Repair and Regeneration 15(4), 450–458 (2007).
40. D. Bularda, R. Șerban, C. Butnaru, M. Mareș, L. C. Burtan, L. Rădulescu, and C. Mârțu, "Searching for a better animal model for chronic tympanic membrane perforation," Journal of Personalized Medicine 14(5), 513 (2024).
41. N. H. Shomer, K. H. Allen-Worthington, D. L. Hickman, M. Jonnalagadda, J. T. Newsome, A. R. Slate, H. Valentine, A. M. Williams, and M. Wilkinson, "Review of rodent euthanasia methods," Journal of the American Association for Laboratory Animal Science 59(3), 242–253 (2020).